Biosensors and Bioelectronics 79 (2016) 280–287

Contents lists available at ScienceDirect

Biosensors and Bioelectronics

journal homepage: www.elsevier.com/locate/bios

Electrosynthesis and characterization of nanostructured polyquinone for use in detection and quantification of naturally occurring dsDNA

Loreto A. Hernández, María A. del Valle *, Francisco Armijo

Pontificia Universidad Católica de Chile, Facultad de Química, Departamento de Química Inorgánica, Laboratorio de Electroquímica de Polímeros (LEP), Vicuña Mackenna 4860, 7820436 Macul, Santiago, Chile

ARTICLE INFO

Article history:
Received 24 September 2015
Received in revised form
10 December 2015
Accepted 15 December 2015
Available online 17 December 2015

Keywords:
Polymer nanowires
Poly(1-amino-9,10-anthraquinone)
Nanowire electrosynthesis
DNA quantification
Electrochemical DNA sensor

ABSTRACT

The detection of naturally occurring desoxyribonucleic acid (DNA) has become a subject of study by the projections that would generate to be able to sense the genetic material for the detection of future diseases. Bearing this in mind, to provide new measuring strategies, in the current work the preparation of a low-cost electrode, modified with poly(1-amino-9,10-anthraquinone) nanowires using a SiO_2 template, is carried out; the assembly is next modified by covalently attaching ssDNA strands. It must be noted that all this is accomplished by using solely electrochemical techniques, according to methodology developed for this purpose. SEM images of the modified surface show high order and homogeneity in the distribution of modified nanowires over the electrode surface. In turn, after the hybridization with its complementary strand, the voltammetric responses enable corroborating the linear relationship between hybridization at different DNA concentrations and normalized current response, obtaining a limit of detection (LOD) $5.7 \cdot 10^{-12}$ g L^{-1} and limit of quantification (LOQ) $1.9 \cdot 10^{-11}$ g L^{-1}. The working dynamic range is between $1.4 \cdot 10^{-7}$ and $8.5 \cdot 10^{-9}$ g L^{-1} with a correlation coefficient 0.9998. The successful obtaining of the modified electrode allows concluding that the high order reached by the nanostructures, guides the subsequent single strand of DNA (ssDNA) covalent attachment, which after hybridization with its complementary strand brings about a considerable current increase. This result allows foreseeing a guaranteed breakthrough with regard to the use of the biosensor in real samples.

1. Introduction

Technological advances in recent years have enabled putting at our disposal tools for developing new bio-recognition techniques, focusing primarily on obtaining DNA biosensors (Drummond et al., 2003), seeking to create devices possessing high sensitivity and selectivity that can contribute in the medical diagnosis field, specifically, expecting that the development of these new methods makes possible the early detection and quantification of various cancers at the cellular level. In turn, an exhaustive study of genome has been accomplished (Man et al., 2015; Rasheed and Sandhyarani, 2014; Wang et al., 2015).

Amidst the variety of sensors developed in the last decade, the optical type stand out through the use of molecules, such as the avidin-biotin interaction (Sassolas et al., 2008), that helps to immobilize the double-stranded bicatenary chains (dsDNA) of a target with a bounded limited number of bases, using external markers *e.g.* ferrocene (Zhao et al., 2014). Thus, LOD down to 10^{-13} mol L^{-1} have been reported (Chung et al., 2011; Dupont-Filliard et al., 2004). In addition, to a lesser extent, works that use surface plasmon resonance achieving LOD 10^{-9} mol L^{-1} have been obtained, but they also need to employ target of bounded bases (10–30 bases per target), to improve their sensitivity and analytical characteristics (Bandyopadhyay and Sarkar, 2014; Zhang et al., 2012).

To obtain bio-sensors with the already mentioned sensory features, electrochemical measuring techniques have become very important, developing all kind of electronic devices for DNA detection, since they enable transducing biochemical signal into electrical response in a readable, low cost and highly sensitive manner (Chen et al., 2012; Man et al., 2015; Paleček and Bartošík, 2012). Electrodes used for these purposes, such as graphite or gold (Zeng et al., 2015), stand out among the wide range of electrode surfaces and, especially, those modified with conductive polymers (CPs), due to the advantages they present, namely high conductivity, biocompatibility, thermal and environmental stability and easy obtainment at low cost (Adhikari and Majumdar, 2004; Heinze et al., 2010).

In recent years, our working group, with extensive experience

* Corresponding author.
E-mail address: mdvalle@uc.cl (M.A. del Valle).

http://dx.doi.org/10.1016/j.bios.2015.12.041
0956-5663/

in this kind of electrodes, has focused on a thorough study of CPs nucleation and growth mechanisms (Romero et al., 2013; Schrebler et al., 1997), in order to achieve their direct nano-structuring on noble or steel electrodes, decreasing thus the production cost. Besides, our group was the first in obtaining polymeric nanowires using just electrochemical technique. Nanowires 2–30 nm diameter were obtained, depending on the substrate used and the synthesized polymer (del Valle et al., 2009; Hernández et al., 2015). Thus, CPs nano-structuring denoted an increase and improvement of the characteristics, in addition to providing better electrochemical responses due to the considerable increase of its effective area. Their use as electro-analytical sensor seems thus quite promising (del Valle et al., 2012; Salgado et al., 2014), with the significant advantage of its high reproducibility in obtaining the so modified electrodes since the electrochemical techniques enable effective control of the experimental variables during the fabrication of the electrode modified with nano-structures generated directly *in situ*.

In this work assembling of a dsDNA electrochemical sensor, based on previously published work, is reported, where the modification of steel electrodes (SS) was achieved utilizing a copolymer of poly(1-amino-9,10-anthraquinone-co-*o*-phenylenediamine) (Poly(1AAQ-*co*-OPD)) (Hernandez et al., 2013), upon which poly(1-amino-9,10-anthraquinone) (P1AAQ nw) nano-wires (Hernández et al., 2015), which remain attached perpendicularly to the electrode surface, have been electrosynthesized. Presently, these nanowires have been covalently modified with ssDNA of biological origin, assessing its use to sense the complementary strand and to establish their quantification parameters.

2. Material and methods

2.1. SS electrode modification with copolymer (SS|cop) and then with template (SS|cop-(tp))

All solutions were prepared with fresh Milli-Q grade water obtained from a Heal Force (Smart Series) deionizer. The experiments were conducted at room temperature (20 °C) under a high purity argon atmosphere in a three-compartment, three-electrode anchor-type electrochemical cell. A 0.07 cm^2 geometric area stainless steel (SS) disc (AISI 316) was used as working electrode, and a platinum wire coil of large geometric area, was the counter electrode. Ag|AgCl in a solution of tetramethylammonium chloride, whose potential matched that of a saturated calomel electrode (SCE) was the reference electrode (East and del Valle, 2000). The monomers used in the electropolymerizations were 1-amino-9,10-anthraquinone (1AAQ, 98%, Aldrich), and *o*-phenylenediamine (OPD, 99.5%, Aldrich), prepared following the protocols reported elsewhere (Hernandez et al., 2013). The template was prepared in an ethanol (98%)/milli-Q water (50% v/v) mixture containing 0.05 mol L^{-1} of potassium nitrate (KNO_3, Aldrich) as supporting electrolyte, 0.0034 mol L^{-1} tetraethyl orthosilicate (TEOS, Aldrich) as precursor of silicon oxide (SiO_2) and 0.115 mol L^{-1} hexadecyltrimethylammonium bromide (CTAB, Aldrich) as surfactant, by applying a fixed potential of −1.400 V for 5 s, and then dried for 12 h at 130 °C.

2.2. P1AAQ nanowire electrosynthesis on SS|cop-(tp)

The P1AAQ nanowire-modified electrodes (SS|cop-nw) have been obtained on SS|cop-(tp) modified electrodes using amperometric method. Nanowires growth inside template nano-channels was conducted by applying 1100 mV during 40 s to the SS|cop-(tp) electrode immersed into a 0.01 mol L^{-1} 1AAQ solution. Subsequently, the device was dried during 12 h at room temperature. Removal of the SiO_2 template from SS|cop-nw electrodes was conducted using a 0.1 mol L^{-1} NaOH (99.0%, Merck) solution. To this purpose, 10 μL was deposited on each electrode and allowed to stand for 10 min. The solution was then neutralized and the electrode washed with 5% w/w $NaHCO_3$ (99%, Merck). This extraction procedure is repeated twice for each device (Hernández et al., 2015).

2.3. Covalent modification of SS|cop-nw with ssDNA

Electrosynthesis of (SS|cop-nw-ssDNA) sensors was carried out using a dsDNA solution extracted from a 0.15 g L^{-1} fish sperm (Aldrich), diluted with milli-Q water, in a PBS (phosphate buffer saline) of pH 7.3 containing 0.1 mol L^{-1} sodium chloride (NaCl 99.99% w/w, Merck), 2.6 mmol L^{-1} potassium chloride (KCl 99.5% w/w, Merck), 0.04 mol L^{-1} potassium hydrogen phosphate (K_2HPO_4 chloride 99% w/w, Merck) and 0.01 mol L^{-1} potassium dihydrogen phosphate (KH_2PO_4 99.5% w/w, Merck as stock solution. Its actual concentration ($3.2 \cdot 10^{-2}$ mol L^{-1}) was determined using UV–vis spectrometry at 260 nm. From this stock solution, aliquots for preparing solutions of lower concentration are taken.

Nanowires covalent modification with ssDNA strands was conducted employing 200 mL of 0.1 mol L^{-1} imidazole ($C_3H_4N_2$, 99.0% w/w, Merck), 440 mL of dsDNA stock solution, 100 mL of 1-ethyl-3-(3-dimethylaminopropyl)carbodiimide) (EDAC 99.0% w/w, AK Scientific Inc.) in PBS at 80 °C by immersing the modified electrode in this solution for 1 h.

Calibration curves and figures of merit (LOD and LOQ) were obtained using 25 mL of $1 \cdot 10^{-6}$–$1 \cdot 10^{-10}$ g L^{-1} ssDNA solutions, to determine the maximum sensitivity of the working electrode. To construct calibration curves, $7.14 \cdot 10^{-9}$ to $1 \cdot 10^{-7}$ g L^{-1} ssDNA solutions were used. LOD and LOQ were determined from sensitivity curves and blank measurements.

2.4. Instruments

All electrochemical measurements were conducted on a CH750D Instruments Electrochemical Workstation. Images from the electrode surface were obtained on a LEO VP1400 scanning electron microscope (SEM), and on a Hitachi HF2000-FEG transmission electron microscope (TEM), using carbon-coated nickel grids. DNA concentrations were obtained on a UV–vis SPECORD 40 Analytik Jena spectrophotometer. All computations were carried out using the functional density theory (DFT) with 6-311G basis set and the Gaussian 09W software package as favorite program (Gaussian 09 et al., 2009). The methodology involves the optimization of the geometry in the monomer scaling to the 1AAQ pentamer optimizing its structure and energy from a Hartree Fock (HF) level until the use of hybrid functional B3LYP, scaling from bases 6-31 until 6-311G, re-optimizing each time, for each obtained molecule.

3. Results and discussion

3.1. P1AAQ computational studies: Behavior as oLIGOMER and projection as polymer

1AAQ pentamer geometry optimization using the Gaussian 09W computing platform, allowed establishing an approximation of the effective size of the oligomer, in order to project these calculations to the polymer (Fig. 1a). In a previous work (Hernández et al., 2015) it was established by SEM, nanowires of about 30 nm in diameter (Fig. 2b). Therefore, if the optimized diameter of each strand is about 22.712 Å, it may be inferred that each P1AAQ nanowire should consists of about 10–13 strands.

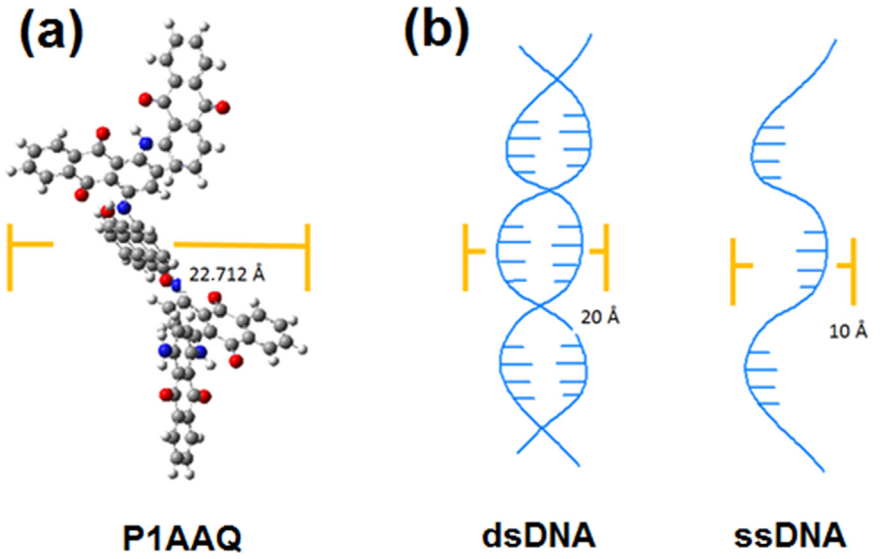

Fig. 1. Optimization of the spatial geometry of 1AAQ pentamer, and comparison of dsDNA and ssDNA.

On the other hand, the ssDNA has a diameter of 10 Å (Richmond and Davey, 2003), therefore covalent immobilization onto each nanowire or the subsequent hybridization with its complementary strand should not be hindered by steric effect. In turn, the nano-structuring of the polymer should allow that a large amount of ssDNA modifies the electrode surface, resulting in low detection limits.

Having in mind that its covalent modification with DNA will be subsequently intended, pentamer diameters were compared with those of ssDNA and dsDNA (Fig. 1), realizing that these possess very close molecular sizes when the DNA is in its bicatenary form.

The computing study therefore enables inferring that, being the polymer nanostructured, it should be quite feasible to have a large amount of dsDNA joined by nanowires, which should result in better electro-analytical response, such as suggested in the current work.

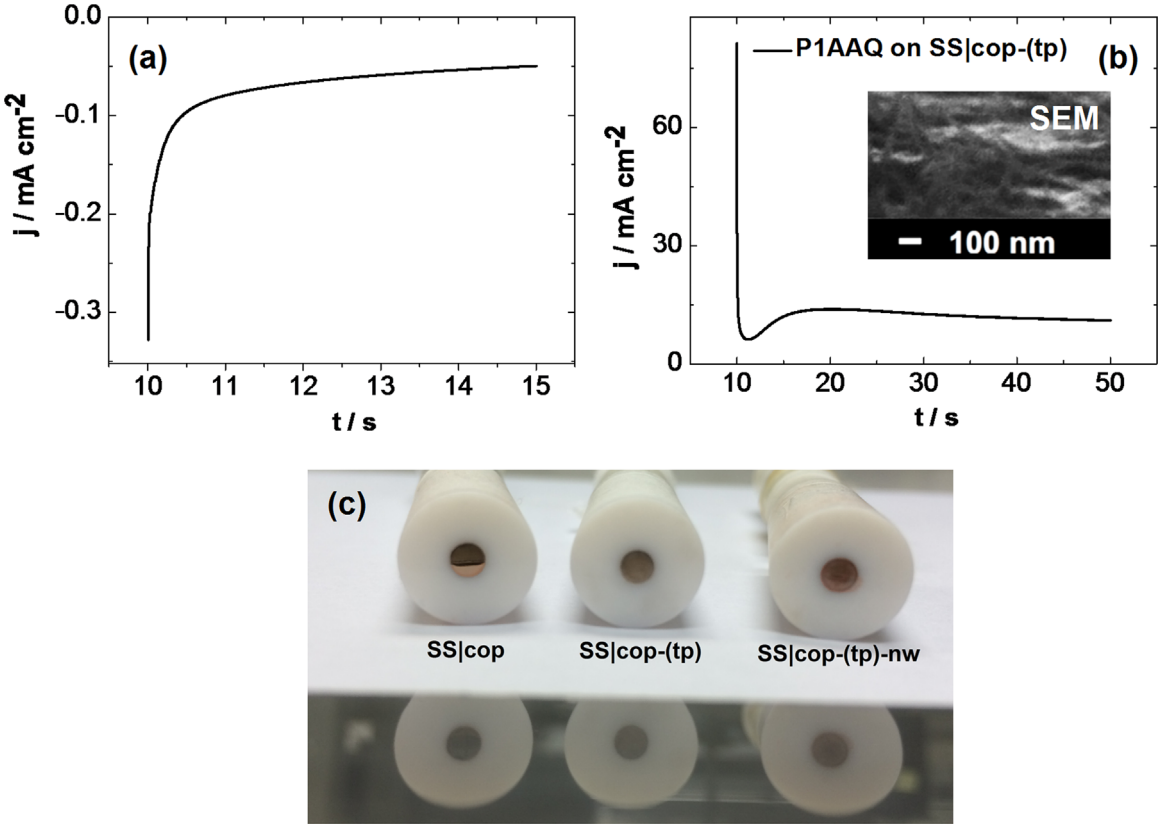

Fig. 2. (a) j/t transient recorded during template electro-obtaining on SS modified with copolymer. Interface: SS|cop 0.0034 mol L^{-1} $(C_2H_5O)_4Si$ + 0.115 mol L^{-1} $C_{19}H_{42}BrN$ + 0.05 mol L^{-1} KNO_3 in ethanol/ Milli-Q water (50% v/v); (b) j/t transient during P1AAQ electro-synthesis on SS|cop-(tp). Interface: SS|cop-(tp) 0.001 mol L^{-1} (1AAQ) + 2 mol L^{-1} H_2SO_4/Milli-Q water (4:1 v/v); (c) disk electrode photographs after each modification step.

3.2. Electrode modification with copolymer (SS|cop), template (SS|cop-(tp)) and P1AAQ nanowires (SS|cop-nw)

SS|cop-nw was prepared according to protocols established in previous works (Hernández et al., 2015). In the first step, a thin film of poly(1AAQ-*co*-OPD) (Hernández et al., 2013) (5 cycles) was electro-synthesized on the SS electrode, to enhance adhesion of the nanowires over the electrode surface modified with a copolymer of chemically related nature that enables modifying the physical adherence of the nanowires upon the metal surface, by means of chemical bonding through the polymer surface, between P1AAQ blocks belonging to the copolymer and P1AAQ nw. Moreover, as demonstrated in previous studies (Hernandez et al., 2015), low roughness allows summing up to the chemical properties, the most suitable physical conditions for nanowires adhesion. This step prior to nanowires electrosynthesis, also responds to the need of having the maximum reproducibility at each stage, due to the multiple steps that follow the subsequent process of covalent modification with ssDNA

On this copolymer film, the mesoporous SiO_2 film was subsequently electro-synthesized by reduction at short times (Walcarius et al., 2007) (Fig. 2a). This coating acts as template for the electrosynthesis of P1AAQ nw (Fig. 2b), obtained after template removal, perpendicularly disposed over the cop surface (30 nm in diameter, 200 nm long), Fig. 2b inset. In Fig. 2c, the modifications on the working electrode can be appreciated, which allows a quick confirmation of the change in each process, evidenced by a bronze color (SS|cop), loss of metallic luster (SS|cop-(tp) and finally a red color, which accounts for the modification of template nanochannels with P1AAQ (SS|cop-(tp)-nw).

3.3. Electrode modification with ssDNA on SS|cop-nw (SS|cop-nw-ssDNA) and hybridization with complementary ssDNA

Biological occurring DNA can be characterized by directly measuring the UV–vis absorption, the purity being established from the A_{260}/A_{280} ratio. Contamination by proteins can be verified this way (a 1.8 ratio reveals a relatively pure matrix). Another absorption that could be indicative of a contaminated sample is that appearing at 230 nm, ascribed to carbohydrates, peptides, phenols and aromatic compounds (for pure samples, A_{260}/A_{230} is 2.2). In Fig. 3a the absorption spectrum obtained for dsDNA in PBS, pH 7.34 stock solution is shown. This spectrum reveals that the commercial dsDNA contains no main interferents such as proteins ($A_{260}/A_{280}=1.82$), but yes molecules of smaller molecular size ($A_{260}/A_{230}=3.1$). However, these should not constitute a major interferent when used as sensor.

On the other hand, in Fig. 3b the response of P1AAQ nw in PBS (pH 7.34) was recorded. The redox couple corresponding to the P1AAQ nw quinone groups, located at P_{ox} 800 mV and P_{red} at 0 mV, is seen.

One major disadvantage when working with commercial DNA, which has been directly extracted from a living source as in this case, is, besides the own contaminants of the obtainment, the problem to make it react since it comes in its more stable form, *i.e.* as double stranded DNA. The protocol to facilitate the de-hybridization involves heating at 80 °C and freezing immediately after 15 min; however, even so is very likely the double helix be re-formed, being unable to have ssDNA effectively in its highest concentration. This is why SS|cop-nw modification was performed hot at 80 °C throughout the process, in order to obtain just ssDNA modified electrodes, not dsDNA.

The voltammetric responses recorded during each of the manufacturing processes, are shown in Fig. 4a.

As shown in Fig. 4a, the electrode modified just with P1AAQ nw exhibits a stable response, evidencing the presence of quinone groups, which, in addition, is consistent with the experimental data found in this study. Following covalent attachment of ssDNA to SS|cop-nw, a decrease of the recorded current is observed, evidencing at first that the electrode was modified with ssDNA, decreasing the conductivity of the nanowire-modified electrode, due to conjugation loss. In addition, it presents monocatenary strands that form tangles, reducing thus the electrolyte diffusion to the electrode, maybe because the active sites become clogged (Fig. 4b), as postulated by Piro et al. (2007). However, it is worth noting that only a current decrease is observed, but the visualization of the redox couple was not missed, a definite evidence of nanowires presence.

Finally, subsequent to hybridization to form dsDNA, a significant current increase was observed, which is consistent with the idea that to generate the bicatenary chain, its formation as a tangle disappears, being now completely linear and normal to the electrode. Consequently, the active sites are again free and the conjugation of the macromolecule reset, showing up as a current increase, as schematically depicted in Fig. 4b.

3.4. SS|cop-nw-ssDNA SEM images

SEM characterization of the ssDNA-modified electrodes is shown in Fig. 5, where the micrographs obtained with different degrees of magnification (Fig. 5a–d.), are observed for the SS|cop-nw-ssDNA electrode. These images were obtained after the

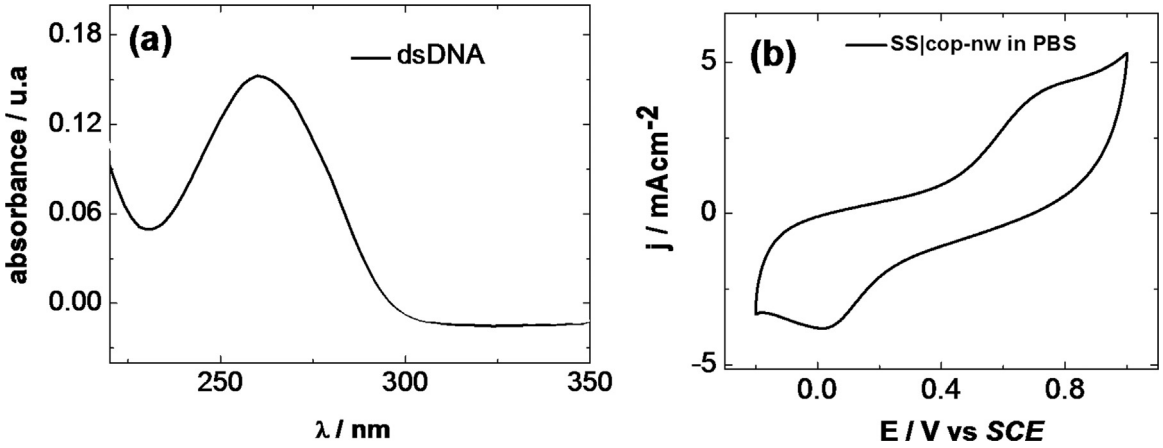

Fig. 3. (a) dsDNA UV–vis spectrum in PBS, pH 7.34; (b) redox response of the P1AAQ nw modified electrode in PBS. Interface: SS|cop-nw in PBS, pH 7.34. Scan rate, $\nu=100$ mV s^{-1}.

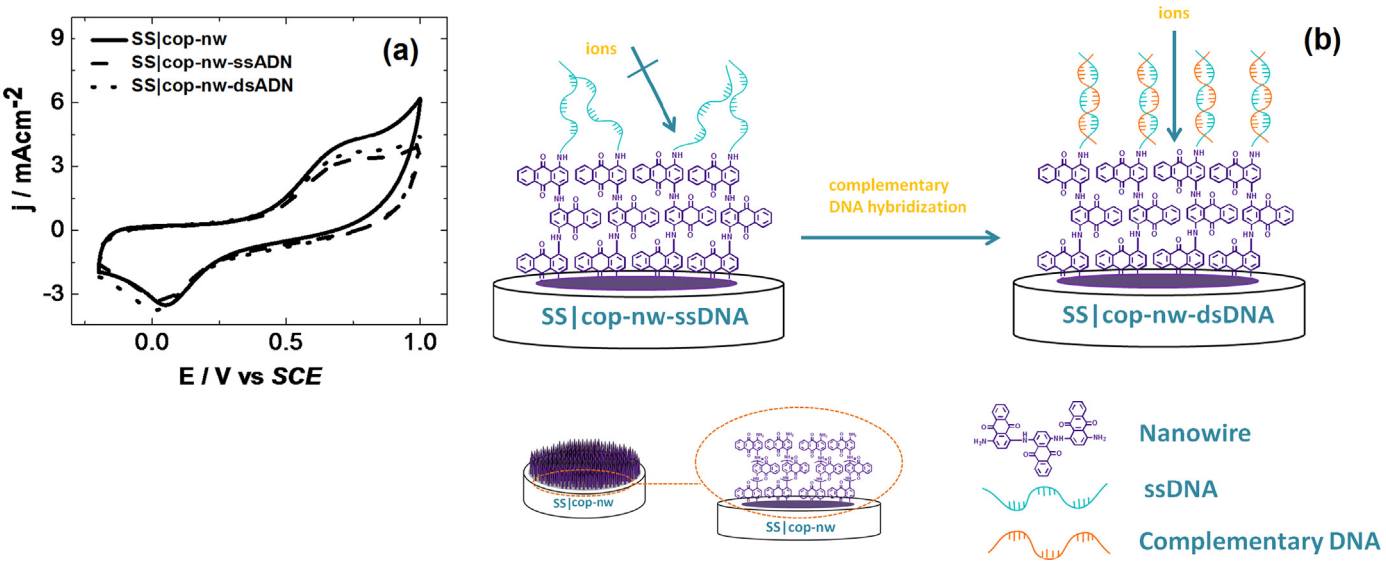

Fig. 4. (a) Voltammetric responses after the three fundamental steps of the nw covalent modification with ssDNA. Interfaces: SS|cop-nw, SS|cop-nw-ssDNA and SS|cop-nw-dsDNA in PBS pH 7.34. $\nu = 100$ mV s^{-1}; (b) schematic representation of the spatial disposition of ssADN and dsADN.

electrochemical modification of the SS electrode with P1AAQ nw (Fig. 2b) and were optimized at higher magnifications, to keep the resolution, due to the large agglomerations formed by the re-ordering that seem to have the ssDNA strands on the nanowires. Although the nano-wires in these images virtually disappear, due to the focusing that SEM makes over the surface, a heterogeneous surface, wherein it can be clearly seen that the mounds marked as ssDNA, seem ordered on an uneven surface, of different nature, postulating that these should be the P1AAQ nw, which is also corroborated by the voltammetric responses depicted in Fig. 4.

This would be consistent with theory, because orderly nano-wires would be essential for orienting or guiding the spatiality of ssDNA strands on the electrode, which, as shown in Fig. 5a and b, are arranged in a relatively homogeneous manner, denoting a great structural order. Some authors suggest that a high % GC (guanine-cytosine) content could be the answer to this type of structuring (Smith, 1992; Sun et al., 2010), owing to the formation of a quadruplex structure, thanks to π–π interactions between unhybridized chains. This is clearly observed in the SEM images (Fig. 5c–d), in which it is even possible to observe the nanowires disposed underneath ssDNA, as specifically highlighted in Fig. 5c.

It is also noteworthy the very high reproducibility of the method used here to obtain the nanostructure modified electrode in each of its stages since the voltammetric responses are always

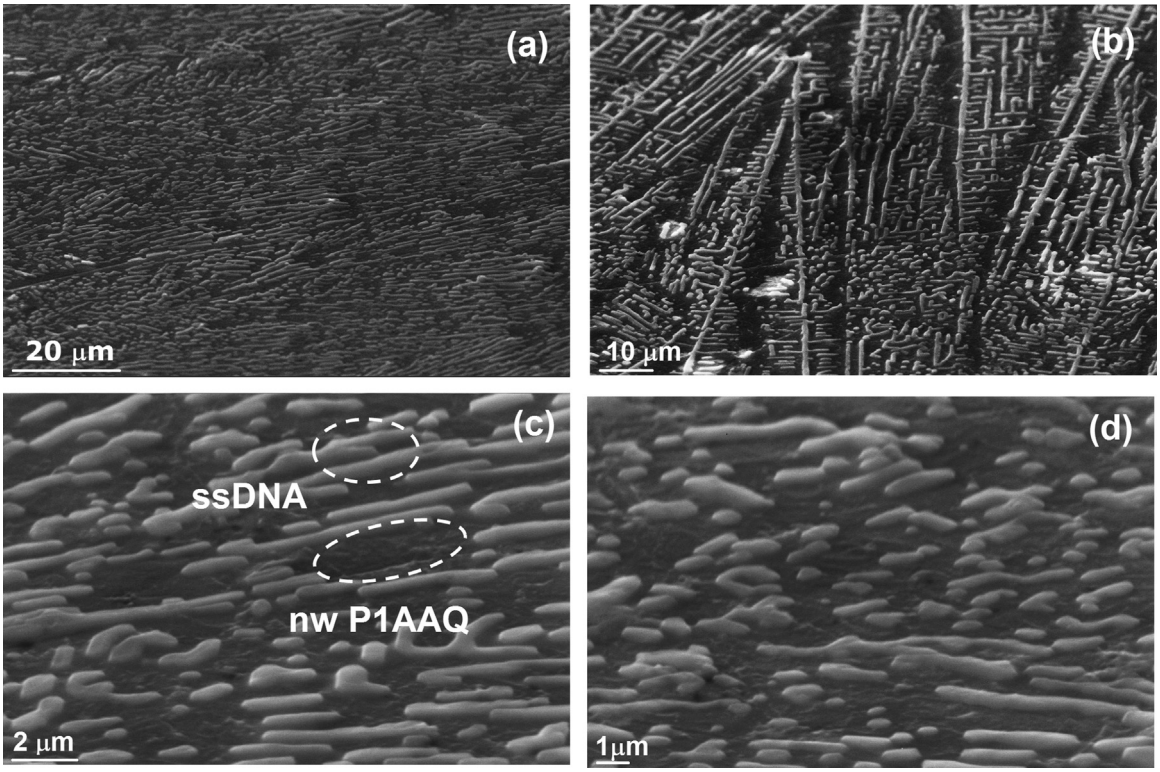

Fig. 5. SS|cop-nw-ssADN SEM images with magnifications (a) 20; (b) 10; (c) 2 and (d) 1 μm.

the same, as are the SEM images. This has been ascribed to the total control of the experimental parameters allowed by the electrochemical techniques as well as by the electrosynthesis of the nanostructures directly over the electrode surface, which gives a significant advantage to this methodology as compared to those that require the nanostructures to be deposited onto the electrode by an *ex situ* mode.

3.5. SS|cop-nw-ssDNA sensor

3.5.1. Data processing methodology: Current normalization

Normalization methodologies become fundamental in obtaining figures of merit that are consistent with the concentrations to be measured in this study ($\leq 1 \cdot 10^{-8}$ g L^{-1}). Although the reproducibility in obtaining voltammetric responses in a first stage of the study (SS|cop-nw) exhibited low standard deviation, the variability of the amperometric response can be a predominant factor in developing an analytical model. Consequently, data processing is accomplished using descriptive statistics, helping to normalize responses and, hence, decreasing the variability of the abovementioned effects.

The normalization applied to each data consists in dividing each obtained value (current) by the total area under the j/t transient. Thus, the new plots will always have area equal to unity, varying its response, by comparison between electrodes, as a result of the various contributions that will have a direct effect just on the amount of dsDNA placed on each device. Data between different electrodes can thus be compared, knowing his answer is always referred to a common area for both sensors that will depend on the intensity of the signal, which, in turn, depends on the amount of P1AAQ-nw interacting with ssDNA.

3.5.2. dsDNA chrono-amperometric determination

Fig. 6a shows transients recorded during the chrono-amperometric determination of hybridization on the SS|cop-nw-ssDNA working electrode in a dynamic range between $1 \cdot 10^{-6}$ and $1 \cdot 10^{-10}$ g L^{-1}. Measurement of each current was conducted in a PBS solution with electrodes that were subjected to a hybridization process at different ssDNA concentrations.

After applying a constant potential of 0.8 V for 200 s, corresponding to the oxidation peak of the voltammetric response of the SS|cop-nw-dsDNA modified electrode (Fig. 4a), it was verify that it was possible to detect solutions with dsDNA concentration down to $1 \cdot 10^{-10}$ g L^{-1} (Fig. 6a). This result is even more significant considering that in this case the advantage of using DNA of biological origin is already possible, enabling thus to make projections with regard to work with actual samples, unlike what is usually reported, namely working solely with chains of one target of bounded number of bases (Piro et al., 2007; Reisberg et al., 2008).

The choice of the solutions to be evaluated was accomplished from appropriate current responses previously measured for the first dsDNA solution (*solution 1,* $1 \cdot 10^{-6}$ g L^{-1}). The other selected solution were 1.25; 2; 10; 1.000 and 10.000 fold more diluted than *solution 1*, *i.e.* $8 \cdot 10^{-7}$, $5 \cdot 10^{-7}$; $1 \cdot 10^{-7}$; $1 \cdot 10^{-9}$; $1 \cdot 10^{-10}$ g L^{-1}, respectively, to verify the possibility of working at low concentrations, without loss of electrochemical signal. From the obtained results (Fig. 6a) it was observed that the higher the concentration of dsDNA strands attached to the nanowires, the more acceptable the measurements continuity, with low standard deviation as a function of the obtained current, Fig. 6b. However, as dsDNA concentration decreases, it becomes increasingly difficult to achieve greater continuity using chronoamperometric techniques, although is still detectable by this technique, and, besides, the recorded current dispersion is still low. From these results, it was inferred that the lowest concentration to be determined, to guarantee not to be too close of the sensitivity of the proposed analytical method, would be $1 \cdot 10^{-9}$ g L^{-1}.

Fig. 6b depicts the variability during the last 10 s of the recorded amperometric response, which is quite low ($\sigma \leq 10^{-5}$) and, therefore, it is considered that potential application during 200 s is an optimum time for obtaining the current to be normalized.

3.5.3. dsDNA chrono-amperometric quantification

The concentrations used in the calibration curve for ssDNA determination are summarized in Table 1 and the chart and linear regression in Fig. 7.

Statistical analysis of the first linear regression, utilizing standardized concentrations and currents, a first relationship and equation can be obtained that correlates normalized current ($I_{\text{normalized}}$) and concentration. Thus, this first approach to develop an analytical method for ssDNA quantification allowed verifying that the parameters showed an excellent regression line fitting, with correlation coefficient 0.9998, which enables projecting the use of this modified electrode as sensor for ssDNA determination.

The first results concerning the variability obtained for each DNA modification process (σ $I_{\text{normalized}}$ $N=3$) showed the robustness of the method, exhibiting a better reproducibility for the measurements performed in the middle of the curve than at its ends. This can be ascribed to the fact that at low concentrations, near the LOD and LOQ (specified below), a limit of sensitivity exists and, when working on a small area ($3.41 \cdot 10^{-3}$ cm^2) and low

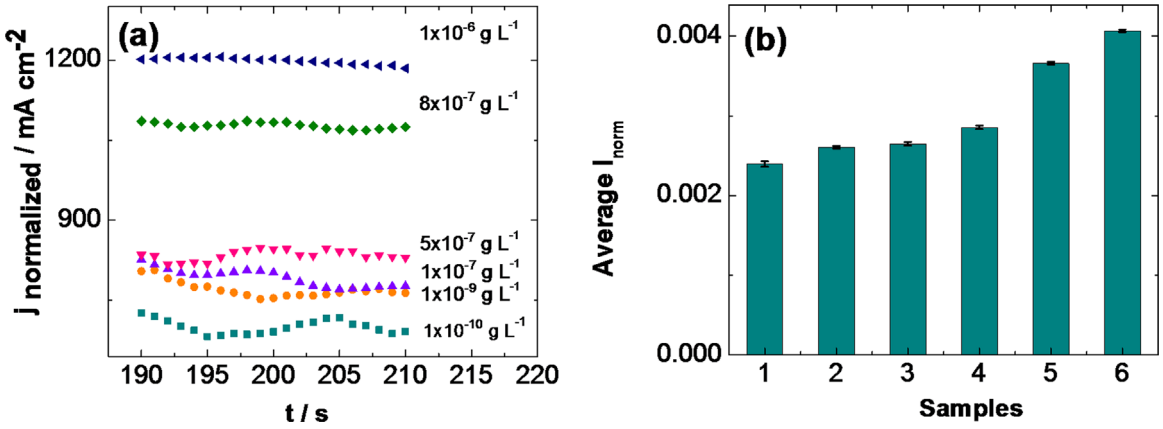

Fig. 6. (a) Chrono-amperometric determination of ssDNA at different concentrations in PBS solution, applying 800 mV for 200 s; (b) standard deviation of the normalized currents for the last 10 s of measurement at the same electrodes in samples (1–6): $1 \cdot 10^{-10}$; $1 \cdot 10^{-9}$; $1 \cdot 10^{-7}$; $5 \cdot 10^{-7}$; $8 \cdot 10^{-7}$ and $1 \cdot 10^{-6}$ g L^{-1}.

Table 1
ssDNA calibration line using SS|cop-nw-ssDNA.

Sample	[ssDNA] (g L^{-1})	$I_{normalized}$ (μA)	σ $I_{normalized}$ (N=3)
1	$8.5 \cdot 10^{-9}$	0.00160 ± 0.00050	$1.84858 \cdot 10^{-4}$
2	$2.0 \cdot 10^{-8}$	0.00189 ± 0.00002	$9.02745 \cdot 10^{-6}$
3	$3.0 \cdot 10^{-8}$	0.00200 ± 0.00020	$6.99206 \cdot 10^{-5}$
4	$8.0 \cdot 10^{-8}$	Out of range	–
5	$1.0 \cdot 10^{-7}$	Out of range	–
6	$1.4 \cdot 10^{-7}$	0.00330 ± 0.00030	$1.16018 \cdot 10^{-4}$

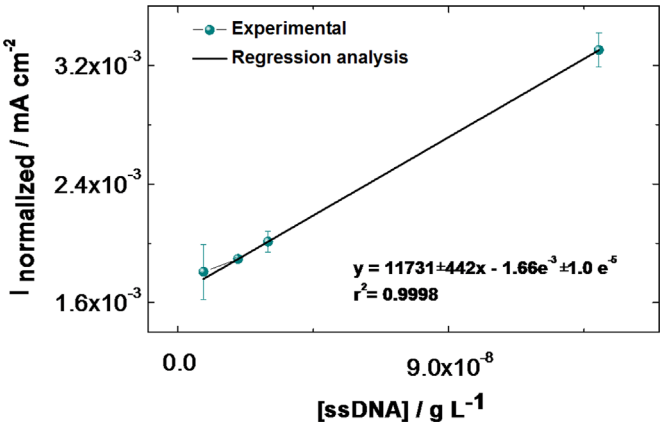

Fig. 7. DNA quantification in PBS (pH 7.34), using the new sensor, applying E=800 mV for 200 s.

Table 2
Figures of merit for quantification of DNA using the new sensor.

Nr. of measurements	X_{blank}	σ_{blank}	LOD (g L^{-1})	LOQ (g L^{-1})
6	$5.1 \cdot 10^{-8} \pm 2.3 \cdot 10^{-8}$	$2.2 \cdot 10^{-8}$	$5.7 \cdot 10^{-12}$	$1.9 \cdot 10^{-11}$

concentrations, more variability in the results is expected. On the other hand, at high concentrations, it may be possible to be working at the limit of the linear range of the method, increasing the variability, as seen in Table 1.

In turn, also in Table 1, two data (4 and 5) were not considered in the calibration curve due to the high variability observed, namely a deviation larger than 30% between data obtained from the line equation and those experimentally found.

In addition, each electrode was utilized on the same and next day of modification. A significant decrease in current was observed, indicating that is essential the measurements be accomplished on the same day of preparation, *i.e.*, with a "fresh" electrode, considering the low stability of the resulting signal. The large number of processes involved in the device fabrication explains this behavior. Nevertheless, thanks to the low cost of the employed materials, their use as disposable device, *i.e.* always fresh, is highly favored.

3.5.4. Determination of DNA sensor analytic parameters

Instrumental figures of merit such as LOD and LOQ, were estimated by measuring six blanks (blank σ $2.23 \cdot 10^{-8}$), using the sensitivity of the plot, without applying $\log_{10}$ to facilitate calculations.

In the near future, it is proposed to work with real samples in the presence of all their interfering contaminant, trying to reproduce the obtained results to validate the method and to project this investigation towards real use in genetic reading devices of fast measuring response and low cost (Table 2).

4. Conclusions

The successful modification of SS electrodes with P1AAQ- nw was accomplished. The process was corroborated by electrochemical and SEM characterization; formation of nanowires with diameter of 30 nm was verified.

Covalent modification of the SS|cop-nw nanostructured surface with ssDNA strands is achieved; subsequently, the later were exposed to its complementary strand, allowing hybridization. This process was checked using voltammetry and SEM imaging.

The obtained sensor possesses a dynamic working range between $1.4 \cdot 10^{-7}$ and $8.5 \cdot 10^{-9}$ g L^{-1} with a correlation coefficient of 0.9998 LOD and LOQ $5.7 \cdot 10^{-12}$ and $1.9 \cdot 10^{-11}$ g L^{-1}, respectively, were found.

The limitations of the sensor increase when working with DNA of natural origin, because of the high dispersion of the length of DNA strands, which hinders the use of the sensor at lower concentrations than those reported here.

Acknowledgments

Funding through FONDECYT Project 1141158 is kindly acknowledged. L.A.H. thanks CONICYT-Chile for a doctoral scholarship folio: 21120127.

References

Adhikari, B., Majumdar, S., 2004. Prog. Polym. Sci. 29, 699–766.
Bandyopadhyay, A., Sarkar, K., 2014. Anal. Biochem. 465, 156–163.
Chen, D., Feng, H., Li, J., 2012. Chem. Rev. 112, 6027–6053.
Chung, D.-J., Kim, K.-C., Choi, S.-H., 2011. Appl. Surf. Sci. 257, 9390–9396.
del Valle, M.A., Gacitúa, M., Díaz, F.R., Armijo, F., Río, Rd, 2009. Electrochem. Commun. 11, 2117–2120.
del Valle, M.A., Gacitua, M., Diaz, F.R., Armijo, F., Soto, J.P., 2012. Electrochim. Acta 71, 277–282.
Drummond, T.G., Hill, M.G., Barton, J.K., 2003. Nat. Biotech. 21, 1192–1199.
Dupont-Filliard, A., Billon, M., Livache, T., Guillerez, S., 2004. Anal. Chim. Acta 515, 271–277.
East, G.A., Del Valle, M.A., 2000. J. Chem. Educ. 77, 97.
Gaussian 09, R.D., Frisch, M.J., Trucks, G.W., Schlegel, H.B., Scuseria, G.E., Robb, M.A., Cheeseman, J.R., Scalmani, G., Barone, V., Mennucci, B., Petersson, G.A., Nakatsuji, H., Caricato, M., Li, X., Hratchian, H.P., Izmaylov, A.F., Bloino, J., Zheng, G., Sonnenberg, J.L., Hada, M., Ehara, M., Toyota, K., Fukuda, R., Hasegawa, J., Ishida, M., Nakajima, T., Honda, Y., Kitao, O., Nakai, H., Vreven, T., Montgomery, J.A., Jr., Peralta, J.E., Ogliaro, F., Bearpark, M., Heyd, J.J., Brothers, E., Kudin, K.N., Staroverov, V.N., Kobayashi, R., Normand, J., Raghavachari, K., Rendell, A., Burant, J. C., Iyengar, S.S., Tomasi, J., Cossi, M., Rega, N., Millam, J.M., Klene, M., Knox, J.E., Cross, J.B., Bakken, V., Adamo, C., Jaramillo, J., Gomperts, R., Stratmann, R.E., Yazyev, O., Austin, A.J., Cammi, R., Pomelli, C., Ochterski, J.W., Martin, R.L., Morokuma, K., Zakrzewski, V.G., Voth, G.A., Salvador, P., Dannenberg, J.J., Dapprich, S., Daniels, A.D., Farkas, Ö., Foresman, J.B., Ortiz, J.V., Cioslowski, J., Fox, D. J. Gaussian, Inc., Wallingford CT., 2009.
Heinze, J., Frontana-Uribe, B.A., Ludwigs, S., 2010. Chem. Rev. 110, 4724–4771.
Hernandez, L.A., del Valle, M.A., Armijo, F.J., Diaz, F.R., Louarn, G., 2013. Electrochemistry 81, 954–960.
Hernández, L.A., del Valle, M.A., Díaz, F.R., Fermin, D.J., Risbridger, T.A.G., 2015. Electrochim. Acta 166, 163–167.
Man, Si. M., Zhu, Q., Zhu, L., Liu, Z., Karki, R., Malik, A., Sharma, D., Li, L., Malireddi, R. K.S., Gurung, P., Neale, G., Olsen, Scott R., Carter, Robert A., McGoldrick, Daniel J., Wu, G., Finkelstein, D., Vogel, P., Gilbertson, Richard J., Kanneganti, T.-D., 2015. Cell 162, 45–58.
Paleček, E., Bartošík, M., 2012. Chem. Rev. 112, 3427–3481.
Piro, B., Reisberg, S., Noel, V., Pham, M.C., 2007. Biosens. Bioelectron. 22, 3126–3131.
Rasheed, P.A., Sandhyarani, N., 2014. Sensor. Actuators B -Chem. 204, 777–782.
Reisberg, S., Piro, B., Noel, V., Nguyen, T.D., Nielsen, P.E., Pham, M.C., 2008. Electrochim. Acta 54, 346–351.
Richmond, T.J., Davey, C.A., 2003. Nature 423, 145–150.
Romero, M., del Valle, M.A., Del Río, R., Díaz, F.R., Armijo, F., Dalchiele, E.A., 2013. J. Electrochem. Soc. 160, G125–G134.
Salgado, R., del Valle, M.A., Duran, B.G., Pardo, M.A., Armijo, F., 2014. J. Appl. Electrochem. 44, 1289–1294.

Sassolas, A., Leca-Bouvier, B.D., Blum, L.J., 2008. Chem. Rev. 108, 109–139.
Schrebler, R., Grez, P., Cury, P., Veas, C., Merino, M., Gómez, H., Córdova, R., Del Valle, M.A., 1997. J. Electroanal. Chem. 430, 77–90.
Smith, F.F.W.J., 1992. Nature 356, 164–168.
Sun, H., Xiang, J., Zhou, Q., Yang, Q., Xu, G., Tang, Y., 2010. Int. J. Biol. Macromol. 46, 123–125.
Wang, W., Fan, X., Xu, S., Davis, J.J., Luo, X., 2015. Biosens. Bioelectron. 71, 51–56.
Zeng, D., Zhang, H., Zhu, D., Li, J., San, L., Wang, Z., Wang, C., Wang, Y., Wang, L., Zuo, X., Mi, X., 2015. Biosens. Bioelectron. 71, 434–438.
Zhang, D., Yan, Y., Li, Q., Yu, T., Cheng, W., Wang, L., Ju, H., Ding, S., 2012. J. Biotechnol. 160, 123–128.
Zhao, W.-W., Xu, J.-J., Chen, H.-Y., 2014. Chem. Rev. 114, 7421–7441.